Supplementary information

In vitro dual activity of *Aloe marlothii* and its chemical constituents against *Plasmodium falciparum* asexual and sexual stage parasites

Sephora Mutombo Mianda [a], Luke Invernizzi[a], Mariëtte E. van der Watt[b,c], Janette Reader[b], Phanankosi Moyo[a,b], Lyn-Marié Birkholtz[b,*], Vinesh J. Maharaj[a,*]

[a] Department of Chemistry, Faculty of Natural and Agricultural Sciences, University of Pretoria, Pretoria 0028, South Africa
[b] Department of Biochemistry, Genetics and Microbiology, Institute for Sustainable Malaria Control, University of Pretoria, Hatfield, Pretoria 0028, South Africa
[c] Institute for Sustainable Malaria Control, School of Health Systems and Public Health, University of Pretoria, Gezina, Pretoria 0031, South Africa

Sephora Mutombo Mianda (sephoramianda@gmail.com)
Luke Invernizzi (lukeinvernizzi@gmail.com)
Mariette E. Botha (mariette.vanderwatt@up.ac.za)
Janette Reader (janette.reader@up.ac.za)
Phanankosi Moyo (phanankosimoyo@gmail.com)
Lyn-Marié Birkholtz (lbirkholtz@up.ac.za)
Vinesh J. Maharaj (vinesh.maharaj@up.ac.za)

*Corresponding author (Chemistry): Vinesh J. Maharaj
Tel: +27 (0824665466)
Email address: vinesh.maharaj@up.ac.za
Department of Chemistry
University of Pretoria
Private Bag x 20
Hatfield, 0028

*Corresponding author (Parasitology): Lyn-Marié Birkholtz
Tel: +27 12 420 2479
Email address: lbirkholtz@up.ac.za
Department of Biochemistry, Genetics and Microbiology
University of Pretoria
Private Bag x 20
Hatfield, 0028

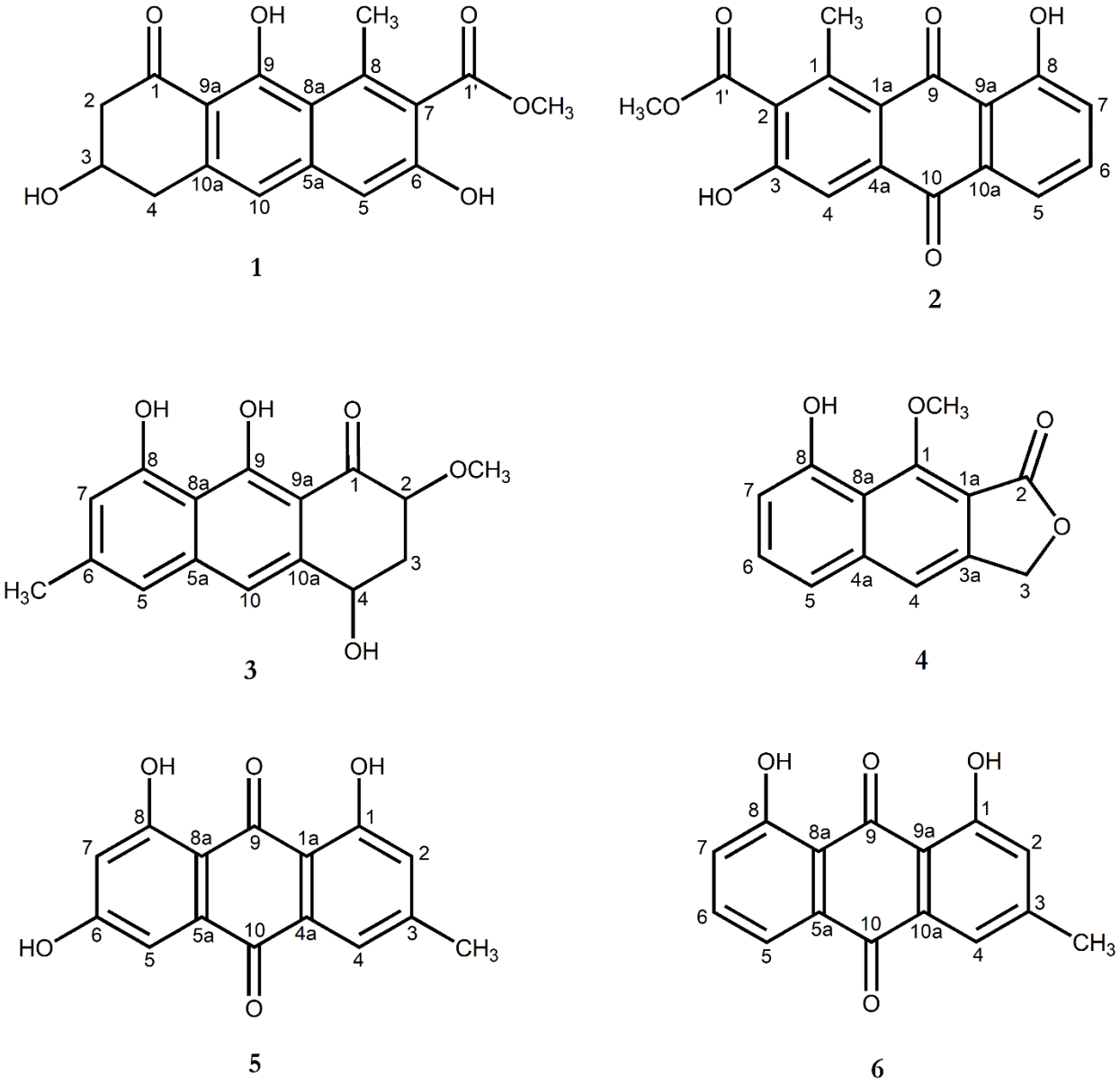

Figure SI.1: Chemical structures of aloesaponol I (**1**), aloesaponarin I (**2**), aloesaponol IV (**3**), β-sorigenin-1-O-methylether (**4**), emodin (**5**), and chrysophanol (**6**).

Supplementary table 1: Analysis of UPLC data of *A. marlothii* roots DCM:MeOH extract run in ESI positive-mode

RT (min)	Acquired $[M+H]^+$ *m/z*	Formula of possible structure	Theoretical $[M+H]^+$ m/z	Calculated accurate mass (Da)	Possible structure	iFit value	MS/MS Data (fragments)	
8.71	317.1104	$C_{17}H_{16}O_6$	317.3139	317.1025	Aloesaponol I	0.001	285.0761	$[M+H]^+$-CH_3OH
							267.0632	$[M+H]^+$-CH_3OH-H_2O
							211.0749	$[M+H]^+$- CH_3OH-H_2O -2CO
9.97	259.1021	$C_{15}H_{14}O_4$	259.2778	259.0970	Prechrysophanol or Aloesaponol II	0.011	241.0855	$[M+H]^+$-H_2O
							195.0797	$[M+H]$+-$2H_2O$-CO
							165.0696	$[M+H]^+$-$2H_2O$-CO-C_2H_6
11.38	313.0786	$C_{17}H_{12}O_6$	313.2822	313.0712	Aloesaponarin I	0.001	281.0435	$[M+H]^+$-CH_3OH
							225.0539	$[M+H]^+$- CH_3OH-2CO
							197.0595	$[M+H]^+$- CH_3OH-3CO
							169.0643	$[M+H]^+$- CH_3OH-4CO

Supplementary table 2: ^{1}H (500 MHz) and ^{13}C (125 MHz) NMR data of isolated aloesaponol I (**1**) in methanol-d_4 compared to the published data (Canche-Escamilla et al., 2019)

Position	**Isolated aloesaponol I (methanol-*D*4)**		**Data published for aloesaponol I (^{1}H, 400 MHz ^{13}C, 100 MHz) (Canche-Escamilla et al., 2019)**	
	δ_H (m, *J* in Hz)	δ_C	δ_H (m, *J* in Hz)	δ_C
1		204.30		204.18
2	2.74 (dd, 7.2, 17.5, 1Ha) 2.97 (d, 7.6, 1Hb)	47.69	2.69 (dd, 16.7, 7.1, 1Ha) 2.95 (dd, 17.2, 3.6, 1Hb)	46.9
3	4.33 (m, 1H)	66.83	4.25 (m, 1H)	64.98
4	2.97 (dd, 3.26, 13.3, 1Ha) 3.2 (dd, 3.26, 15.5, 1Hb)	39.06	2.90 (dd, 15.8, 7.1, 1Ha) 3.12 (dd, 15.8, 3.4, 1Hb)	38.06
5	6.83 (s, 1H)	108.76	6.93 (s, 1H)	108.07
5a		138.13		137.74
6		156.82		155.59
7		139.14		125.95
8		143.07		137.16
8a		111.72		115.88
9		168.00		166.45
9a		117.67		110.76
10	6.87 (s, 1H)	118.18	6.95 (s, 1H)	117.08
10a		126.81		141.32
1’		171.15		168.72
O-CH_3	3.92 (s, 3H)	52.90	3.85 (s, 3H)	52.61
8-CH_3	2.77	21.34	2.70 (s, 3H)	21.06

Supplementary table 3: ^{1}H (500 MHz) and ^{13}C (125 MHz) NMR data of aloesaponarin I (**2**) ($CDCl_3$) compared to the published data (Abdissa et al., 2017).

Position	**Isolated Aloesaponarin I ($CDCl_3$)**		**Data published for Aloesaponarin I (^{1}H, 500 MHz ^{13}C, 125 MHz) (Abdissa et al., 2017)**	
	δ_H (m, *J* in Hz)	δ_C	δ_H (m, *J* in Hz)	δ_C
1		148.10		148.1
1a		121.22		121.2
2		124.63		132.8
3		163.64		162.6
4	7.79 (s, 1H)	115.21	7.80 (s, 1H)	115.2
4a		138.92		138.9
5	7.31 (dd, 1.07, 8.31, 1H)	119.11	7.77 (d, 7.6, 1H)	119.1
6	7.62 (t, 8.10, 1H)	135.97	7.62 (t, 7.6, 1H)	136
7	7.77 (dd, 1.07, 7.50, 1H)	125.18	7.31 (d, 8.2, 1H)	125.2
8		162.61		163.6
9		190.1		189.7
9a		117.64		115.3
10		182.7		182.3
10a		132.77		124.6
1’		170.67		170.7
-OCH_3	4.06 (s, 3H)	53.36	4.06 (s, 3H)	53.3
CH_3	2.97 (s, 3H)	22.04	2.98 (s, 3H)	22
8-OH	12.93 (s, 1H)		12.93 (s, 1H)	

Supplementary table 4: Comparison of ^{1}H (500 MHz) and ^{13}C (125 MHz) NMR data of isolated aloesaponol IV (**3**) in $CDCl_3$ to the published ^{1}H (500 MHz) data in $CDCl_3$ (no record of ^{13}C NMR found in literature) (Yagi et al., 1977).

Position	**Isolated aloesaponol IV ($CDCl_3$)**		**Data published for aloesaponol IV (^{1}H, 500 MHz) (Yagi et al., 1977)**
	δ_H (m, *J* in Hz)	δ_C	δ_H (m, *J* in Hz)
1		201.72	
2	4.44 (dd, 4.41 and 9.6, 1H)	76.59	4.38 (dd, 4 and 8, 1H)
3	2.55 (m, 1H) 2.37 (m, 1H)	36.97	2.3 - 2.5 (m, 2H)
4	5.14 (brs, 1H)	66.95	5.06 (dd, 4 and 6, 1H)
5	6.78 (s, 1H)	113.93	6.71 (d, 1.5, 1H)
5a		144.68	
6		107.19	
7	7.03 (s, 1H)	119.14	6.92 (d, 1.5, 1H)
8		157.95	
8a		139.63	
9		166.49	
9a		137.99	
10	7.14 (s, 1H)	117.45	7.06 (s, 1H)
10a		111.67	
$-OCH_3$	3.68 (s, 3H)	59.30	3.64 (s, 3H)
CH_3	2.46 (s, 3H)	22.35	2.42 (s, 3H)
8-OH	9.59 (s, 1H)		9.51 (s, 1H)
9-OH	15.80 (s, 1H)		15.70 (s, 1H)

Supplementary table 5: ^{1}H (500 MHz) and ^{13}C (125 MHz) NMR data of isolated β-sorigenin-1-*O*-methylether (**4**) compared to the published data (Abegaz and Kebede, 1995).

Position	**Isolated β-sorigenin-1-*O*-methylether ($CDCl_3$)**		**Data published for β-sorigenin-1-*O*-methylether (^{1}H, 300 MHz ^{13}C, 75 MHz) in $CDCl_3$ (Abegaz and Kebede, 1995)**	
	δ_H (m, *J* in Hz)	δ_C	δ_H (m, *J* in Hz)	δ_C
1		157.86		156.54
1a		141.62		141.24
2		168.09		168.22
3	5.38 (d, J =1.2, 2H)	68.94	5.36 (s, 2H)	68.91
3a		110.77		110.49
4	7.56 (s, 1H)	116.51	7.53 (s, 1H)	116.46
4a		116.83		116.83
5	7.38 (d, 8.0, 1H)	119.03	7.35 (br d, 7.7, 1H)	119.07
6	7.52 (t, 8.0, 1H)	131.08	7.52 (t, 7.9, 1H)	131.26
7	6.93 (d, 7.7, 1H)	111.23	6.96 (d, 7.7, 1H)	111.54
8		156.62		156.00
8a		139.99		139.89
$-OCH_3$	4.41 (s, 3H)	65.07	4.45 (s, 3H)	65.16
8-OH	9.73 (s, 1H)		9.76 (s, 1H)	

Supplementary table 6: ^{1}H (500 MHz) and ^{13}C (125 MHz) NMR data of isolated emodin (**5**) in CD_2Cl_2 compared to the published data (Ngan et al., 2017).

Position	**Isolated emodin (CD_2Cl_2)**		**Data published for emodin (^{1}H, 400 MHz ^{13}C, 100 MHz) (Ngan et al., 2017)**	
	δ_H (m, *J* in Hz)	δ_C	δ_H (m, *J* in Hz)	δ_C
1		158.29		161.9
1a		112.94		114.1
2	7.14 (s, 1H)	124.52	7.15 (s, 1H)	124.6
3		149.52		148.4
4	7.73 (s, 1H)	120.80	7.48 (d, 1.2, 1H)	120.9
4a		133.32		133.4
5	7.31 (s, 1H)	129.61	7.06 (s, 1H)	110.4
5a		114.05		135.5
6		157.65		167.7
7	7.30 (s, 1H)	129.52	6.51 (s, 1H)	108.4
8		162.89		165.1
8a		112.65		108.7
9		190.85		189.4
10		186.80		182.2
3-CH_3	2.48 (s, 3H)	22.09	2.41 (s, 3H)	22.0
1-OH	12.11 (s, 1H)		12.12 (s, 1H)	
6-OH	12.98 (s, 1H)			
8-OH	12.29 (s, 1H)			

Supplementary table 7: ^{1}H (500 MHz) and ^{13}C (125 MHz) NMR data of isolated emodin (**5**) in CD_2Cl_2 compared to the published data (Uzun et al., 2020).

Position	**Isolated chrysophanol ($CDCl_3$)**		**Data published for chrysophanol (^{1}H, 400 MHz ^{13}C, 100 MHz) in $CDCl_3$ (Uzun et al., 2020)**	
	δ_H (m, *J* in Hz)	δ_C	δ_H (m, *J* in Hz)	δ_C
1		162.85		162.8
2	7.13 (s, 1H)	124.54	7.07 (s, 1H)	124.5
3		149.52		149.5
4	7.67 (s, 1H)	121.55	7.64 (s, 1H)	121.5
5	7.84 (dd, 1.07, 7.49, 1H)	120.11	7.81 (dd, 1.2, 7.4, 1H)	120.1
5a		133.77		133.75
6	7.69 (t, 8.33, 1H)	137.13	7.67 (dd, 8.4, 7.5, 1H)	137.1
7	7.31 (dd, 1.07, 8.42, 1H)	124.74	7.28 (dd, 1.2, 8.4, 1H)	124.7
8		162.55		162.5
8a		116.01		115.99
9		192.71		192.7
9a		113.87		113.85
10		182.25		182.1
10a		133.40		133.38
-CH_3	2.49 (s, 3H)	22.44	2.46 (s, 3H)	22.4
1-OH	12.05 (s, 1H)		12.01 (s, 1H)	
8-OH	12.16 (s, 1H)		12.12 (s, 1H)	

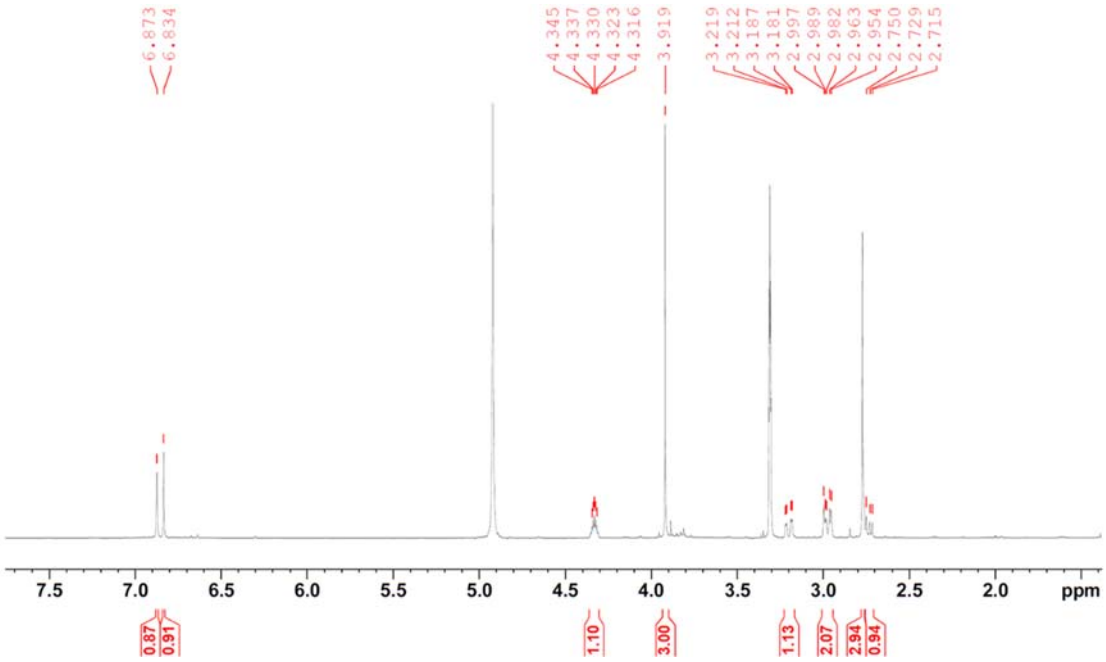

Figure SI.2: ^{1}H NMR (500 MHz, CD_3OD) spectrum of aloesaponol I (**1**)

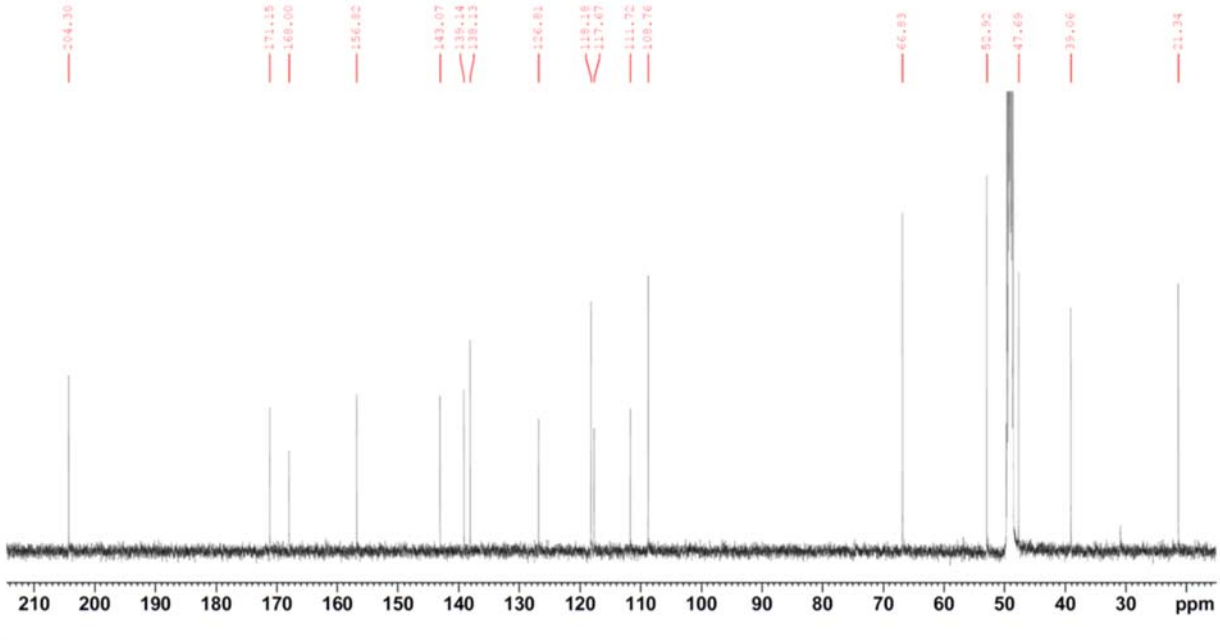

Figure SI.3: ^{13}C NMR (500 MHz, CD_3OD) spectrum of aloesaponol I (**1**)

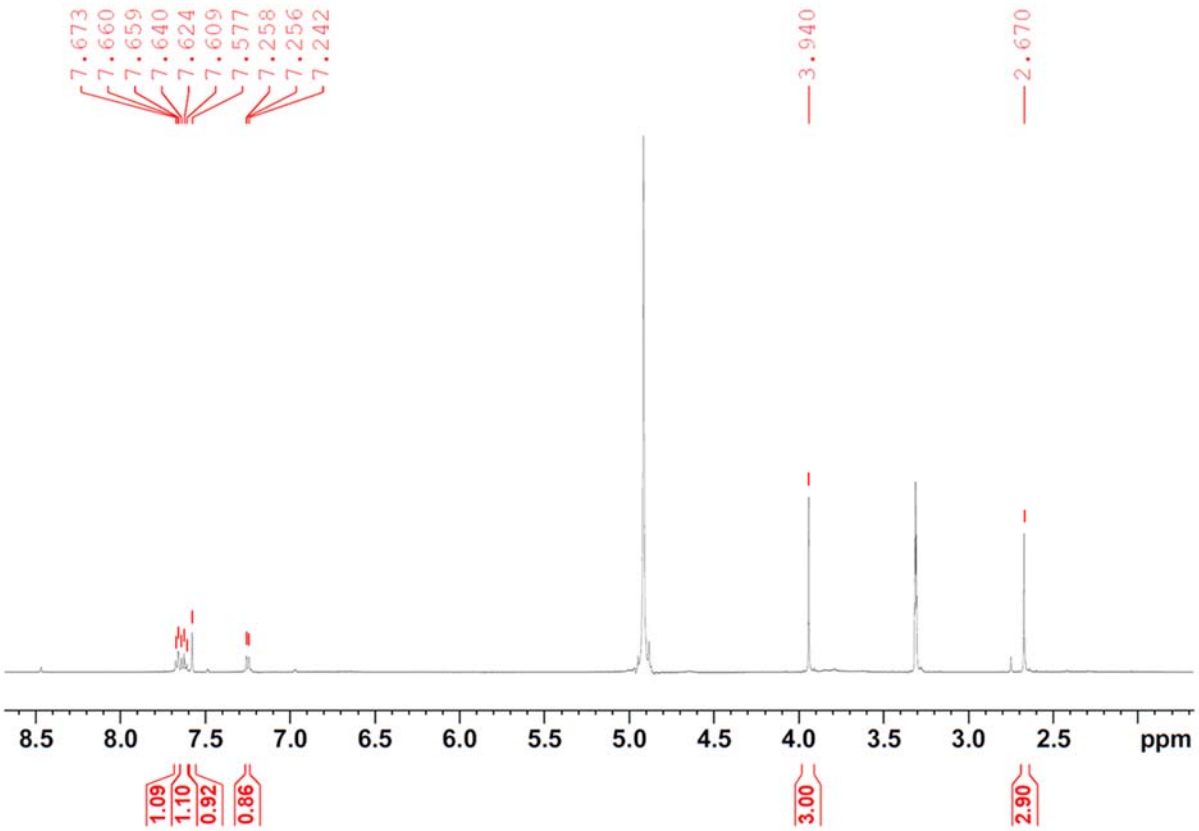

Figure SI.4: 1H NMR (500 MHz, CD_3OD) spectrum of aloesaporarin I (**2**)

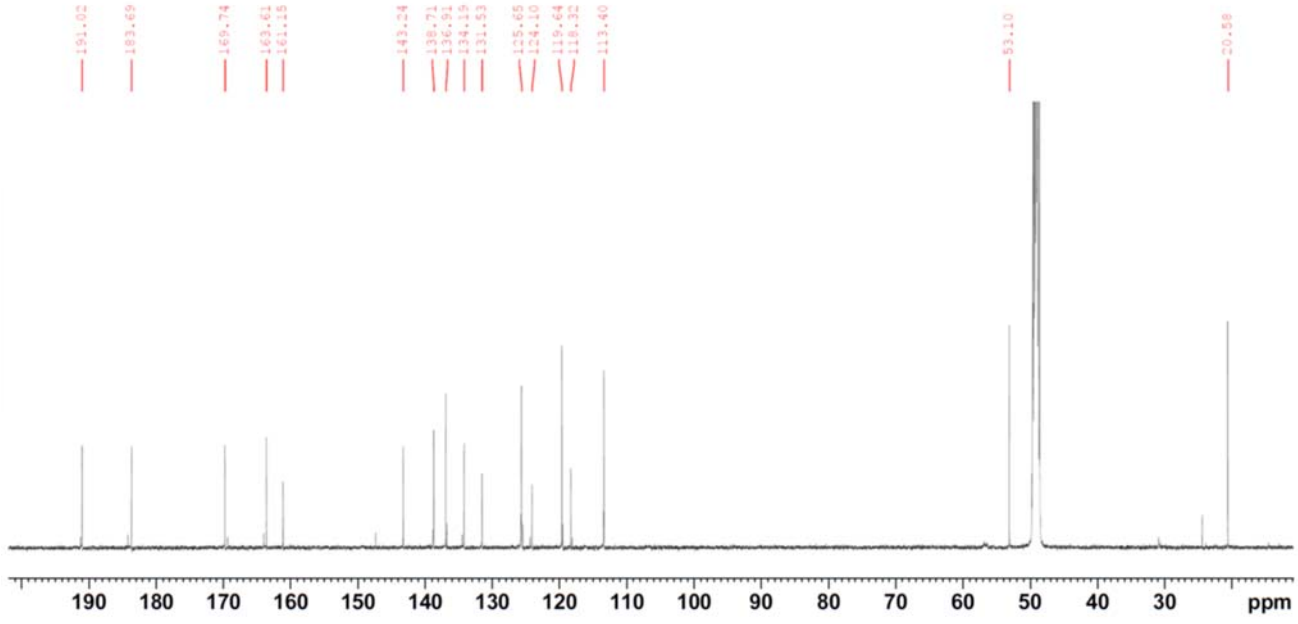

Figure SI.5: ^{13}C NMR (500 MHz, CD_3OD) spectrum of aloesaporarin I (**2**)

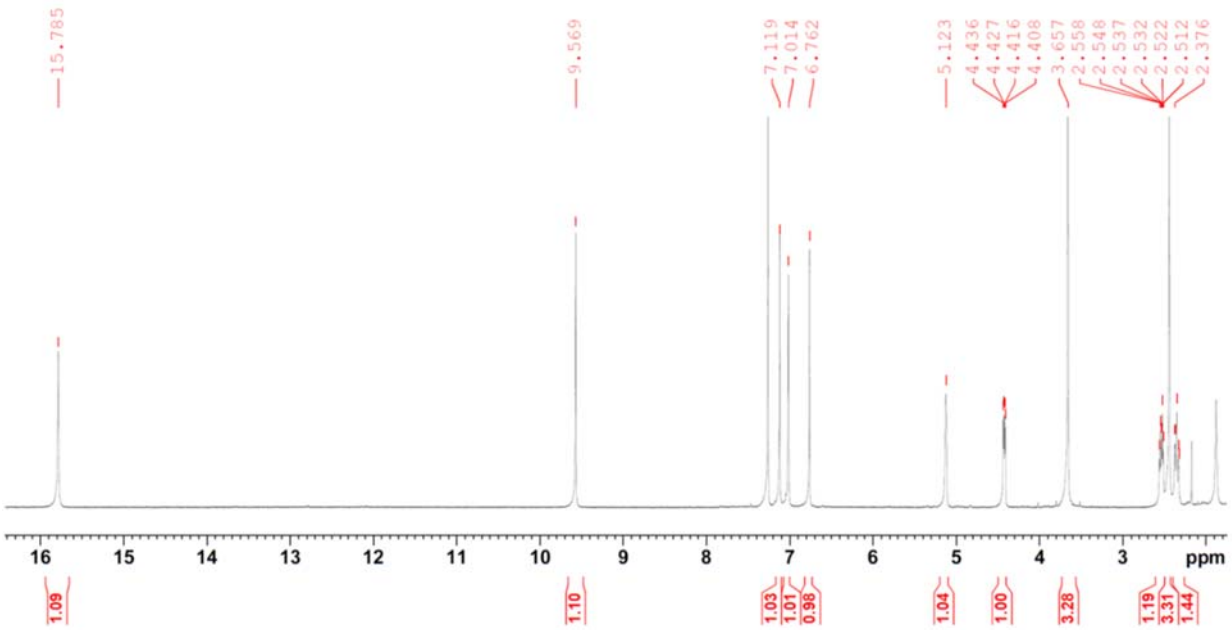

Figure SI.6: ^{1}H NMR (500 MHz, $CDCl_3$) spectrum of aloesaponol IV (**3**)

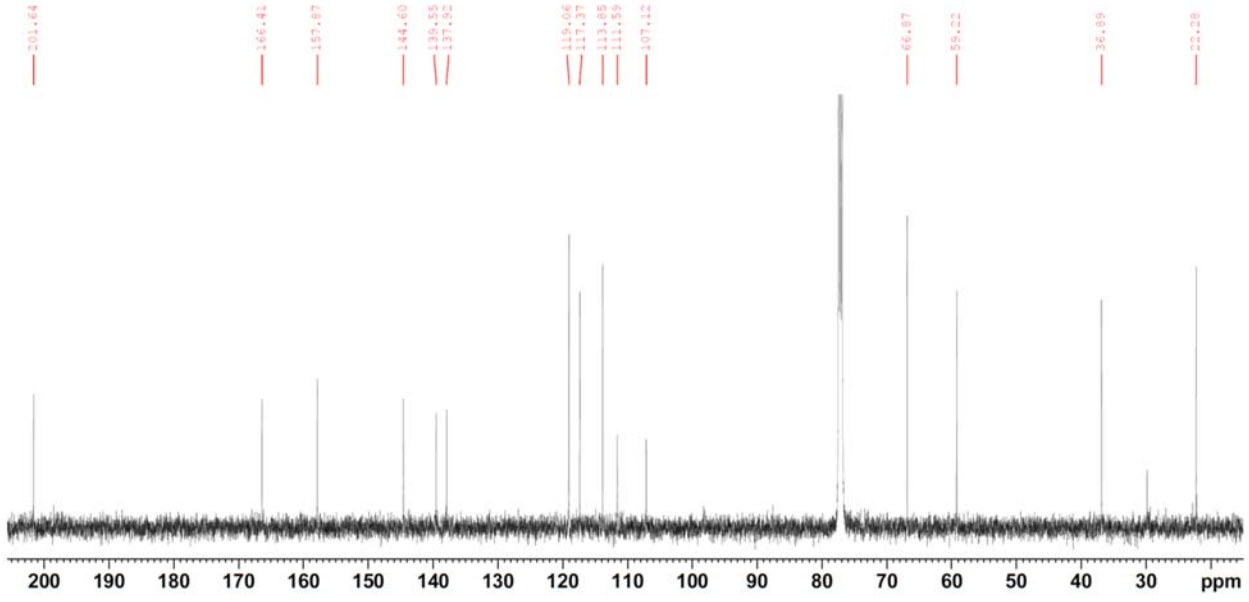

Figure SI.7: ^{13}C NMR (500 MHz, $CDCl_3$) spectrum of aloesaponol IV (**3**)

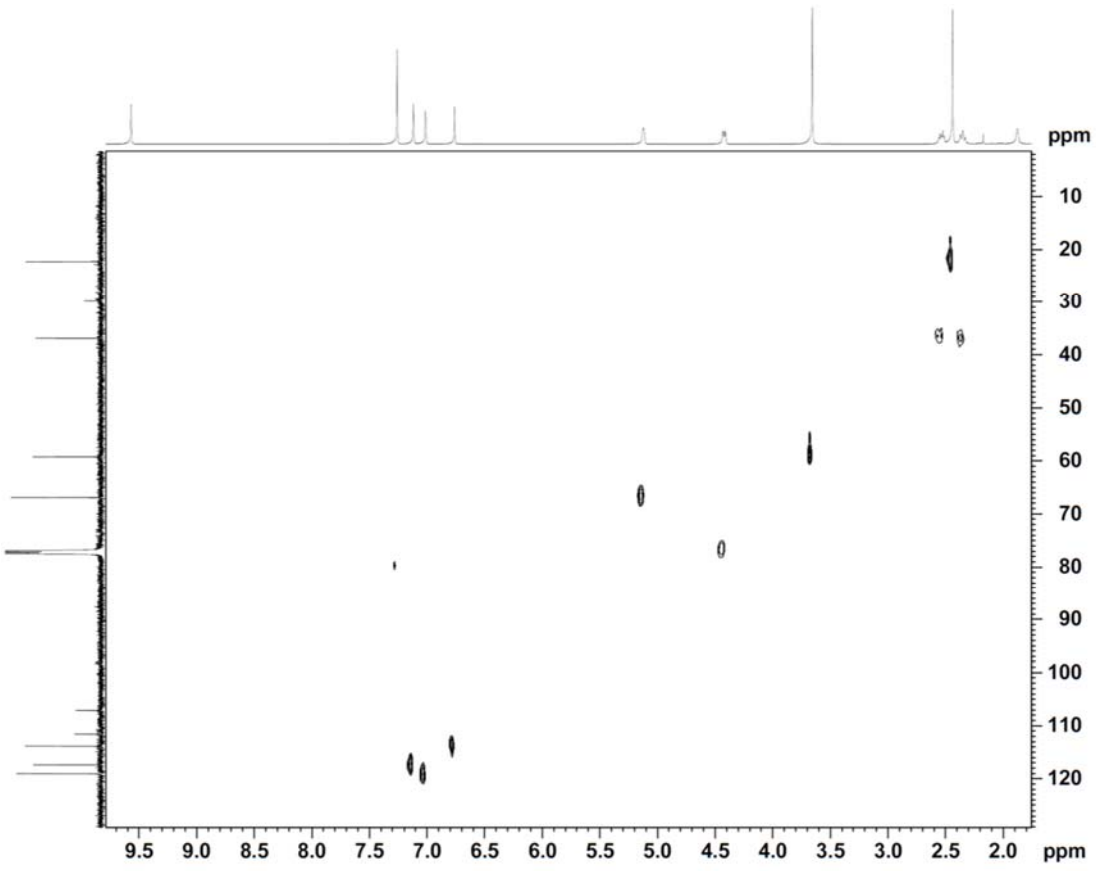

Figure SI.8: HSQC spectrum (500 MHz, $CDCl_3$) of aloesaponol IV (**3**)

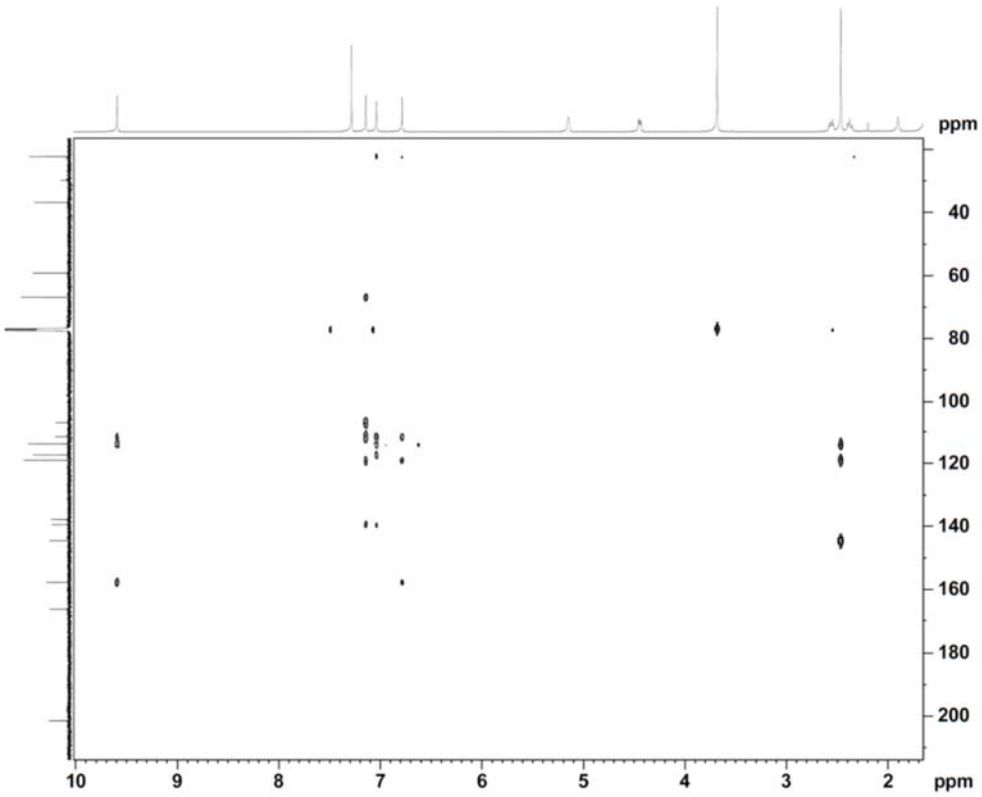

Figure SI.9: HMBC spectrum (500 MHz, $CDCl_3$) of aloesaponol IV (**3**)

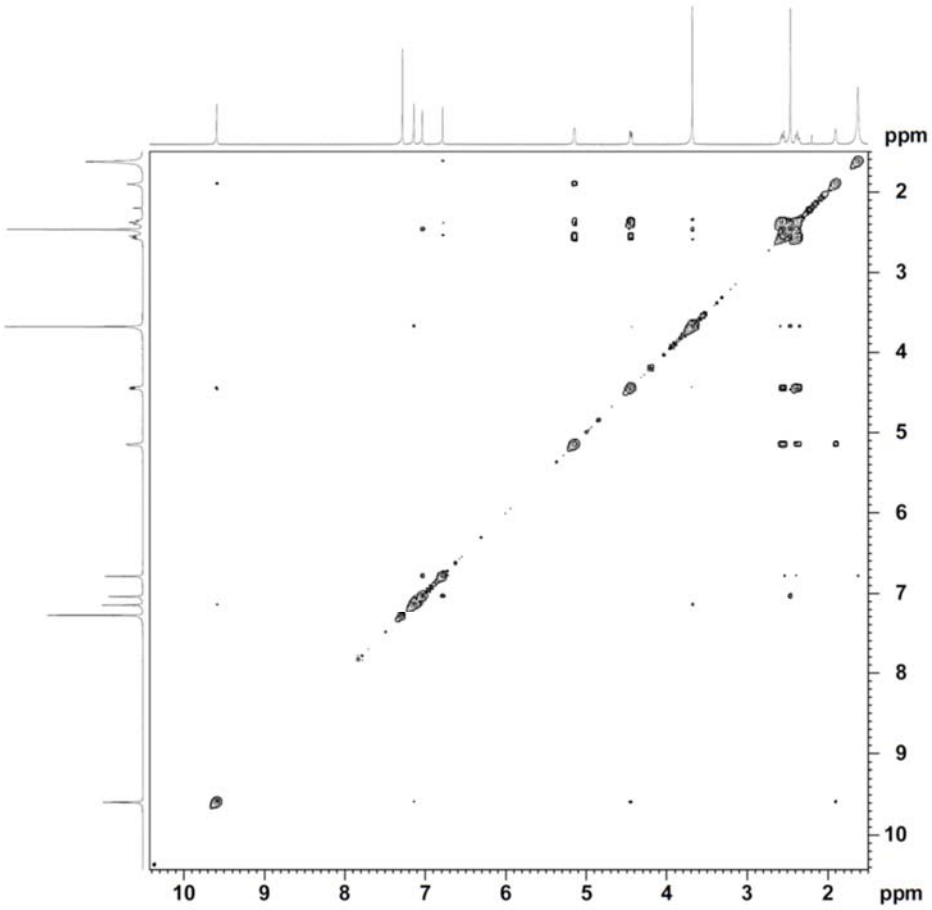

Figure SI.10: COSY spectrum (500 MHz, $CDCl_3$) of aloesaponol IV (**3**)

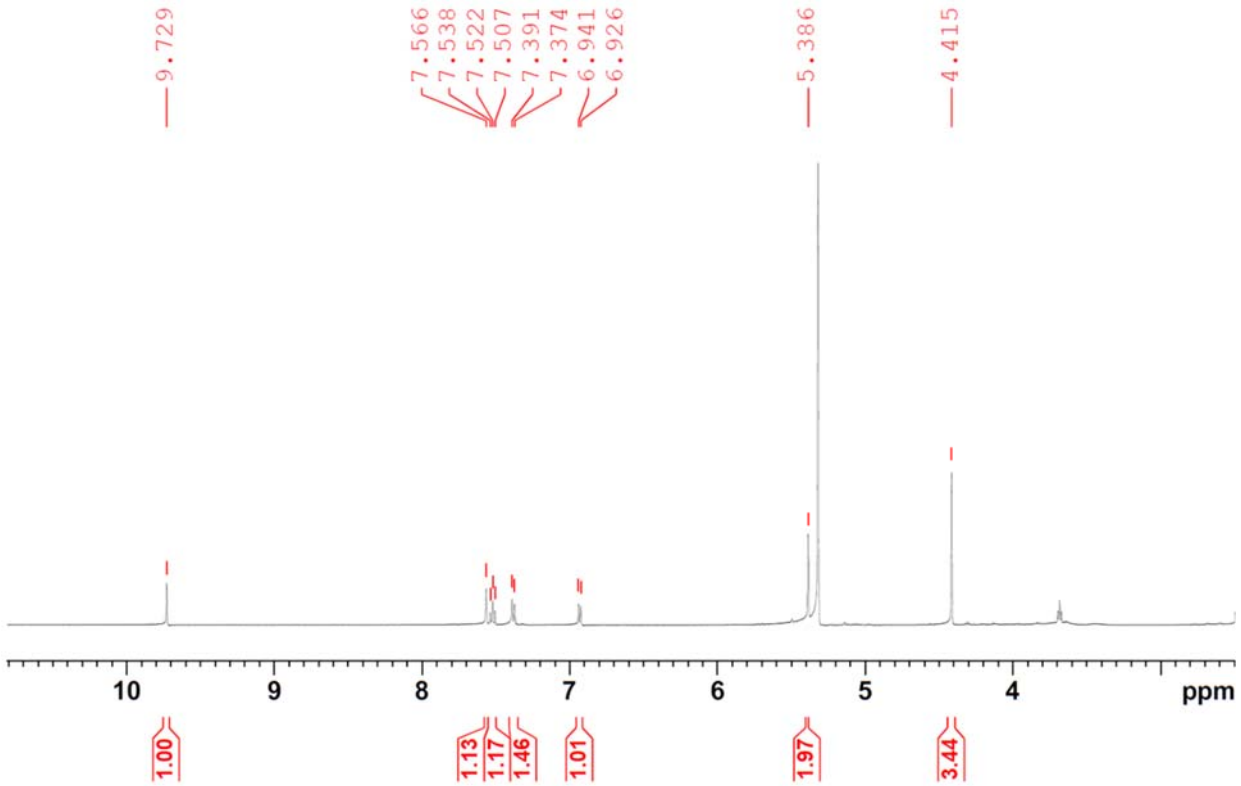

Figure SI.11: ^{1}H NMR (500 MHz, CD_2Cl_2) spectrum of β-sorigenin-1-*O*-methylether (**4**)

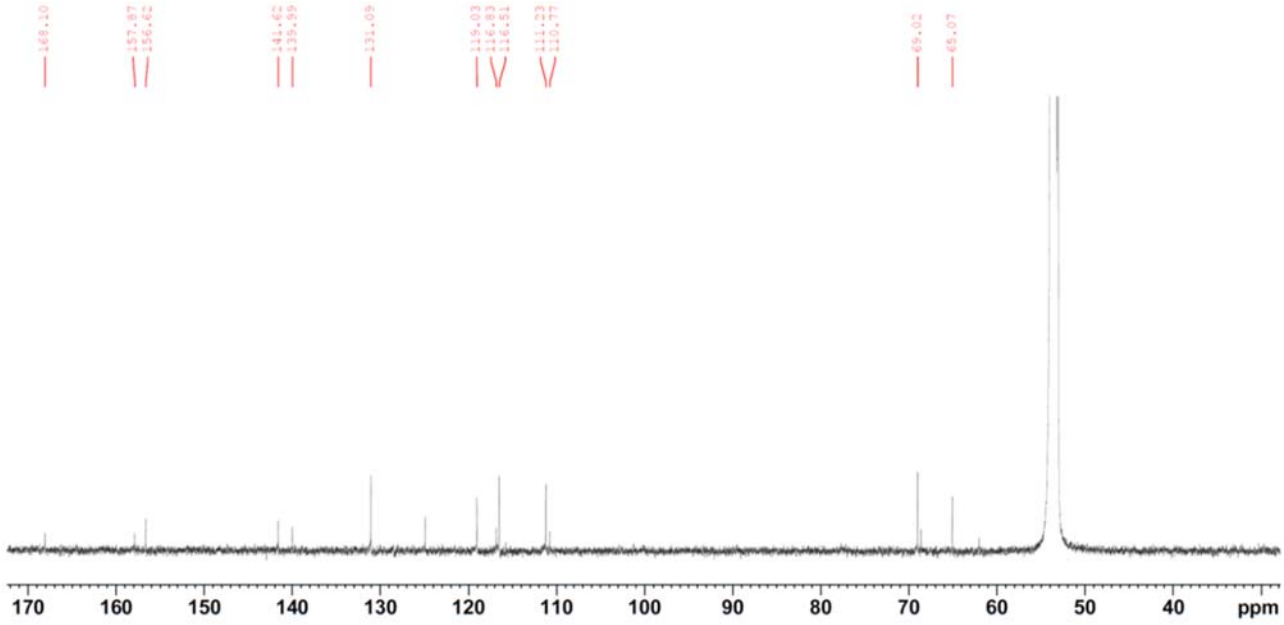

Figure SI.12: ^{13}C NMR (500 MHz, CD_2Cl_2) spectrum of β-sorigenin-1-*O*-methylether (**4**)

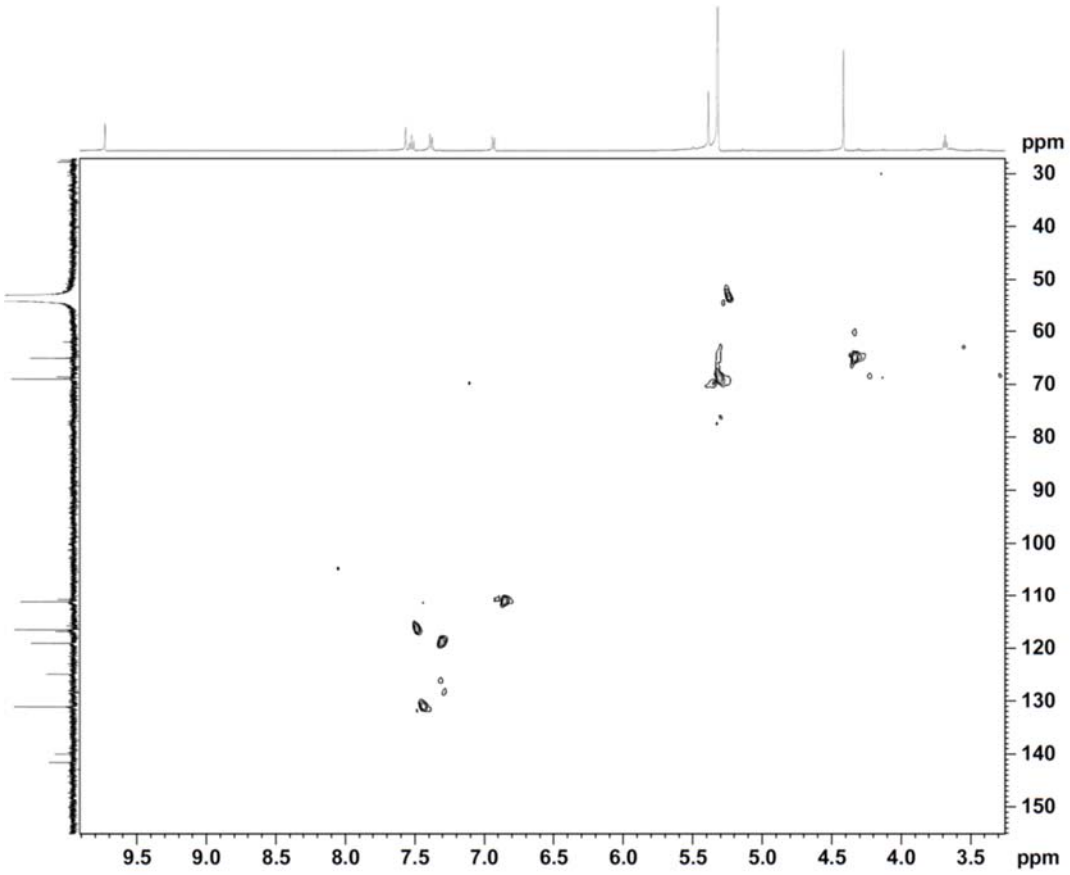

Figure SI.13: HSQC spectrum (500 MHz, CD_2Cl_2) of β-sorigenin-1-*O*-methylether (**4**)

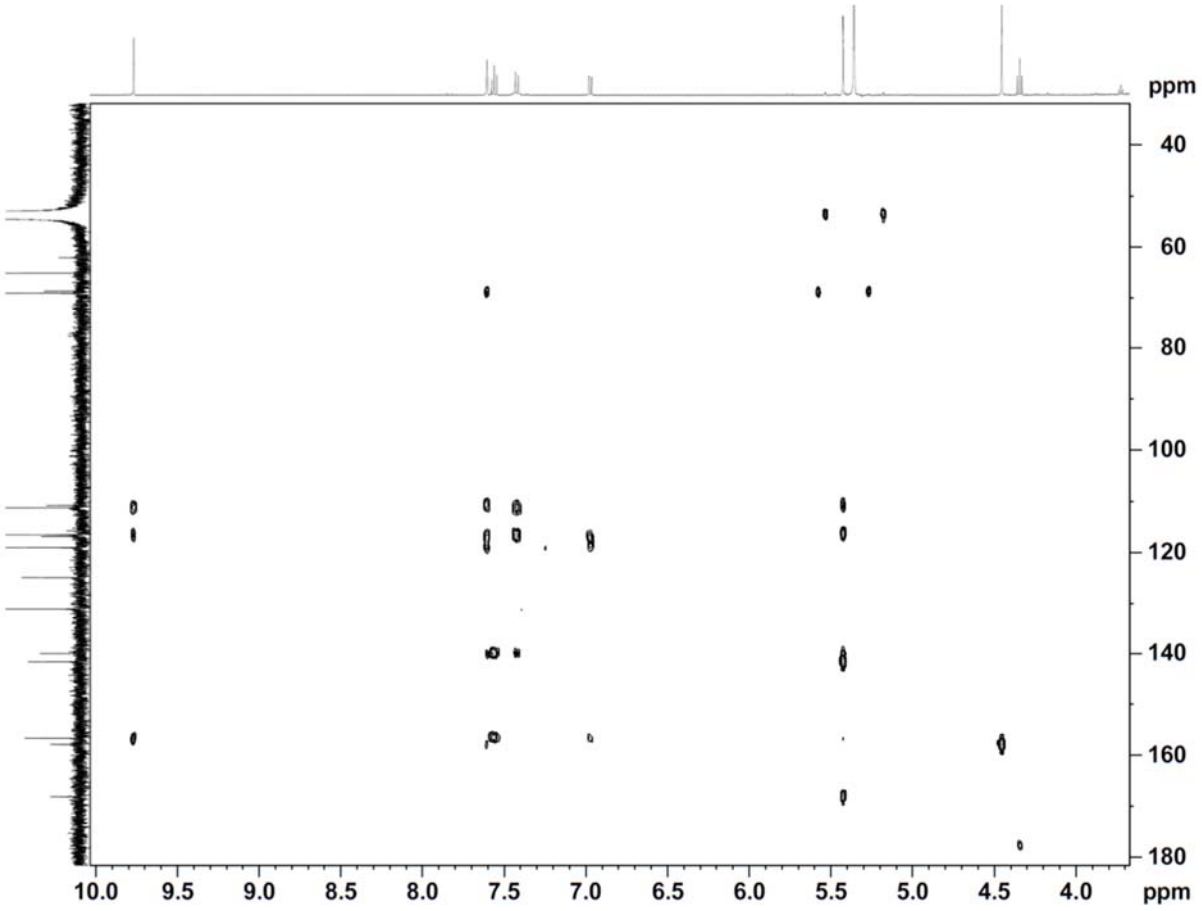

Figure SI.14: HMBC spectrum (500 MHz, CD_2Cl_2) of β-sorigenin-1-*O*-methylether (**4**)

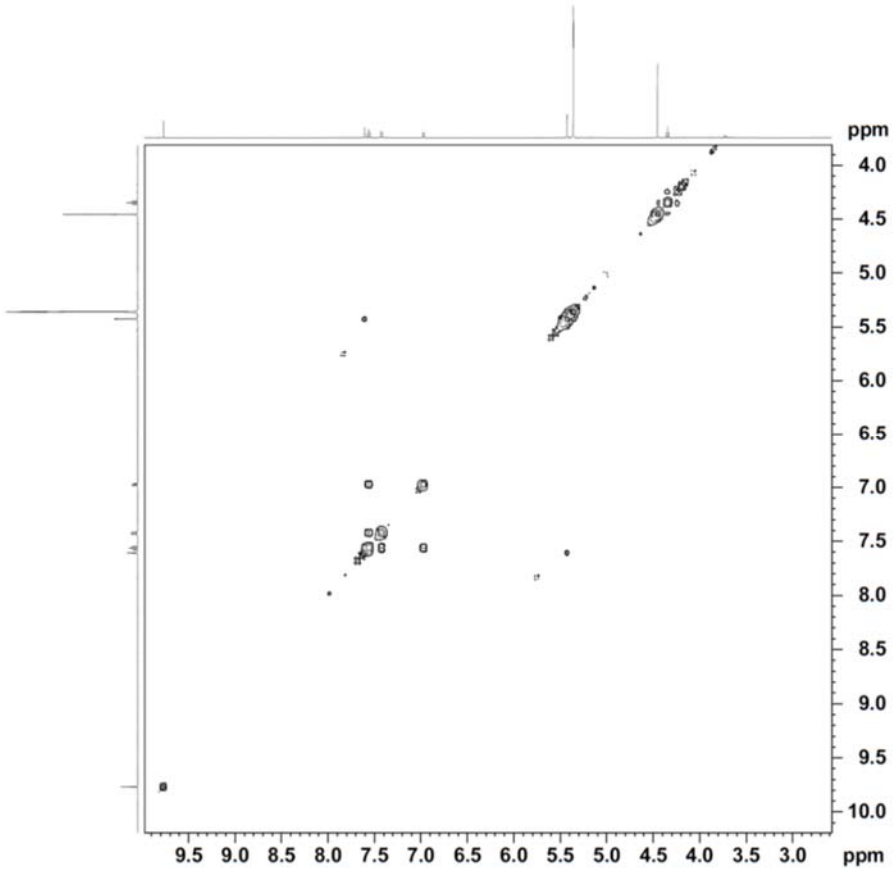

Figure SI.15: COSY spectrum (500 MHz, CD_2Cl_2) of β-sorigenin-1-*O*-methylether (**4**)

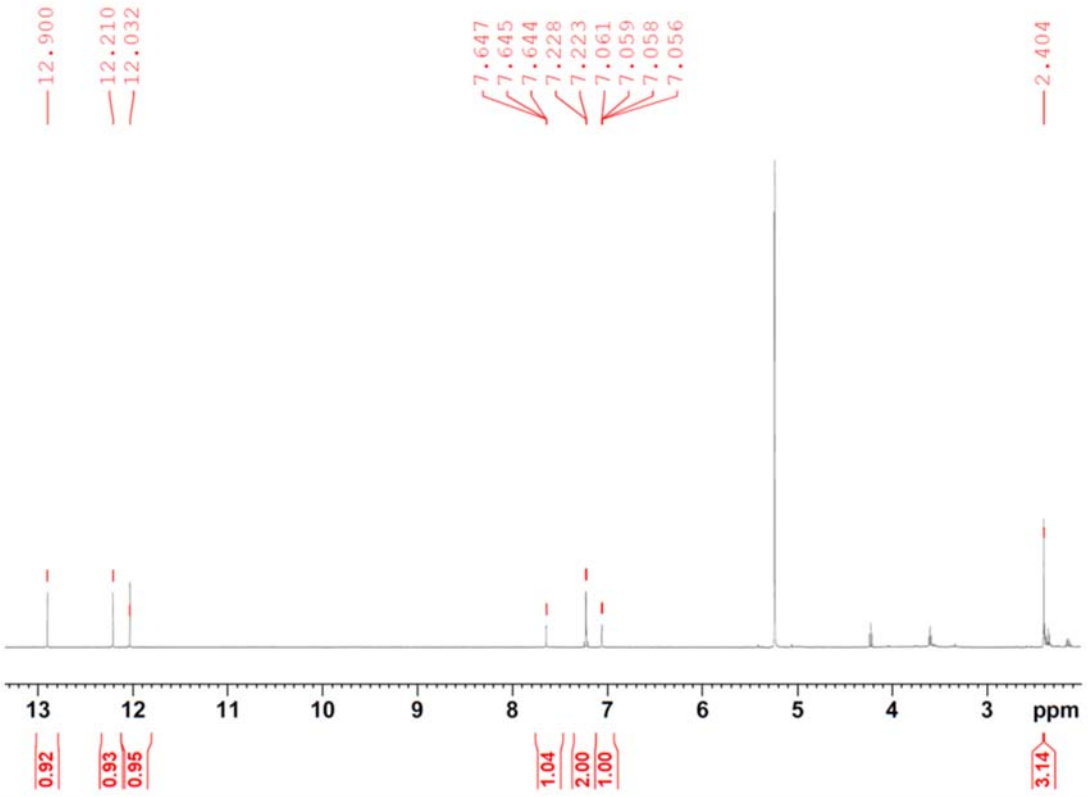

Figure SI.16: ^{1}H NMR (500 MHz, CD_2Cl_2) spectrum of emodin (**5**)

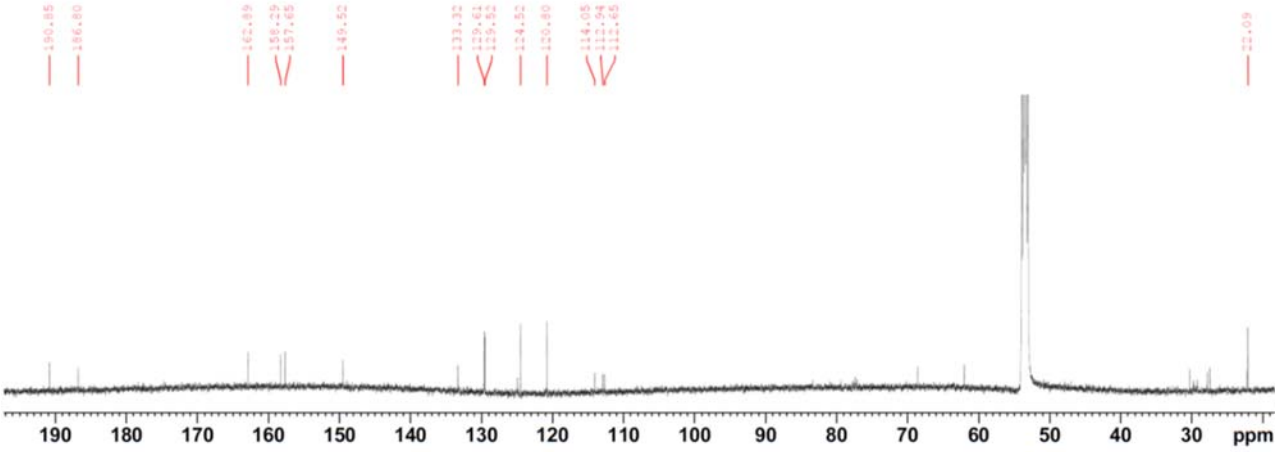

Figure SI.17: ^{13}C NMR (500 MHz, CD_2Cl_2) spectrum of emodin (**5**)

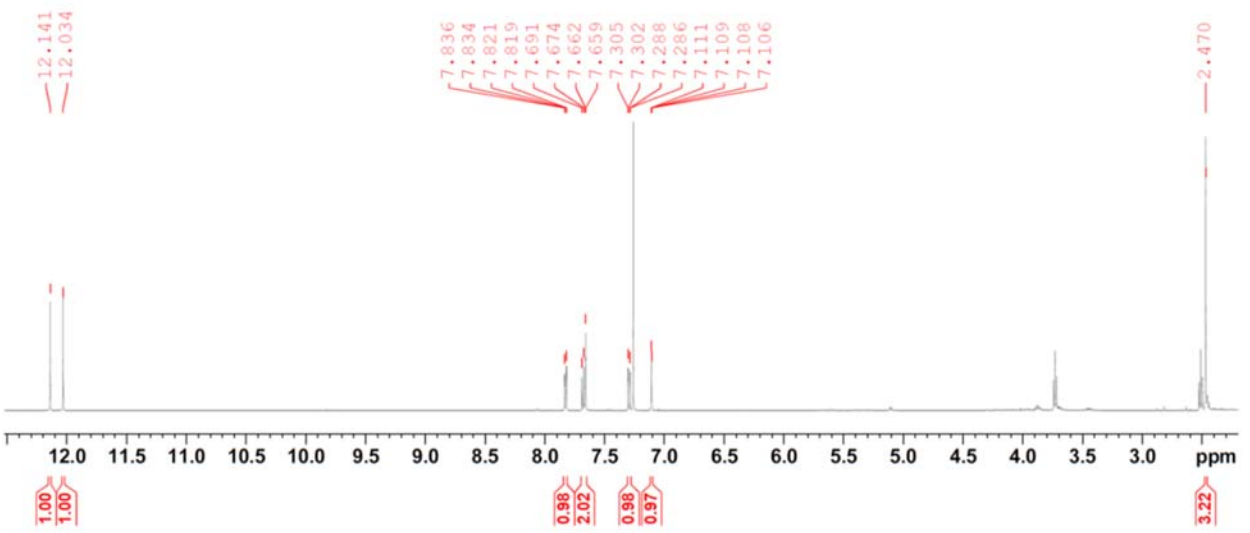

Figure SI.18: ^{1}H NMR (500 MHz, $CDCl_3$) spectrum of chrysophanol (**6**)

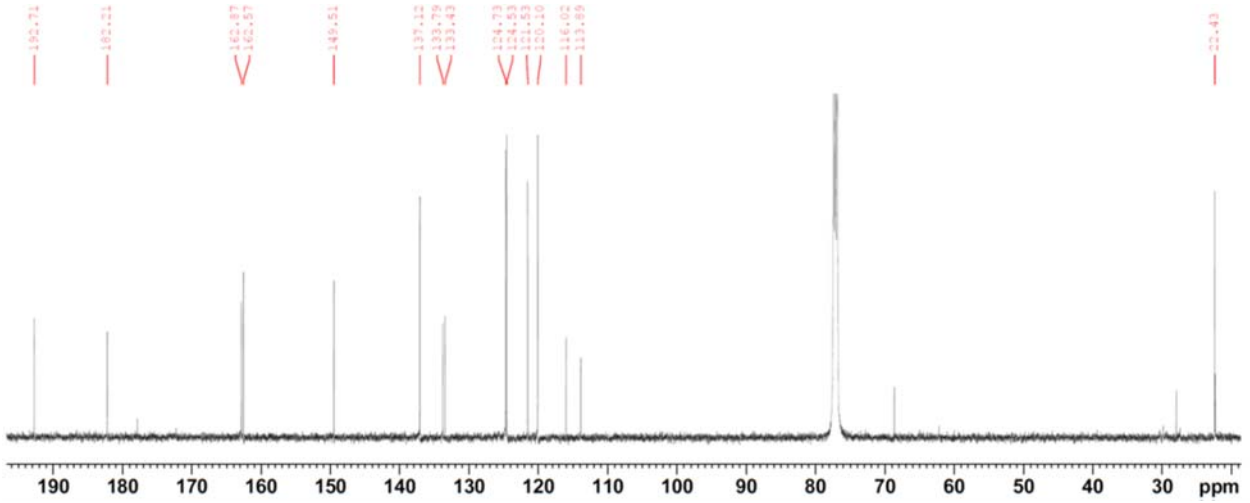

Figure SI.19: ^{13}C NMR (500 MHz, $CDCl_3$) spectrum of chrysophanol (**6**)

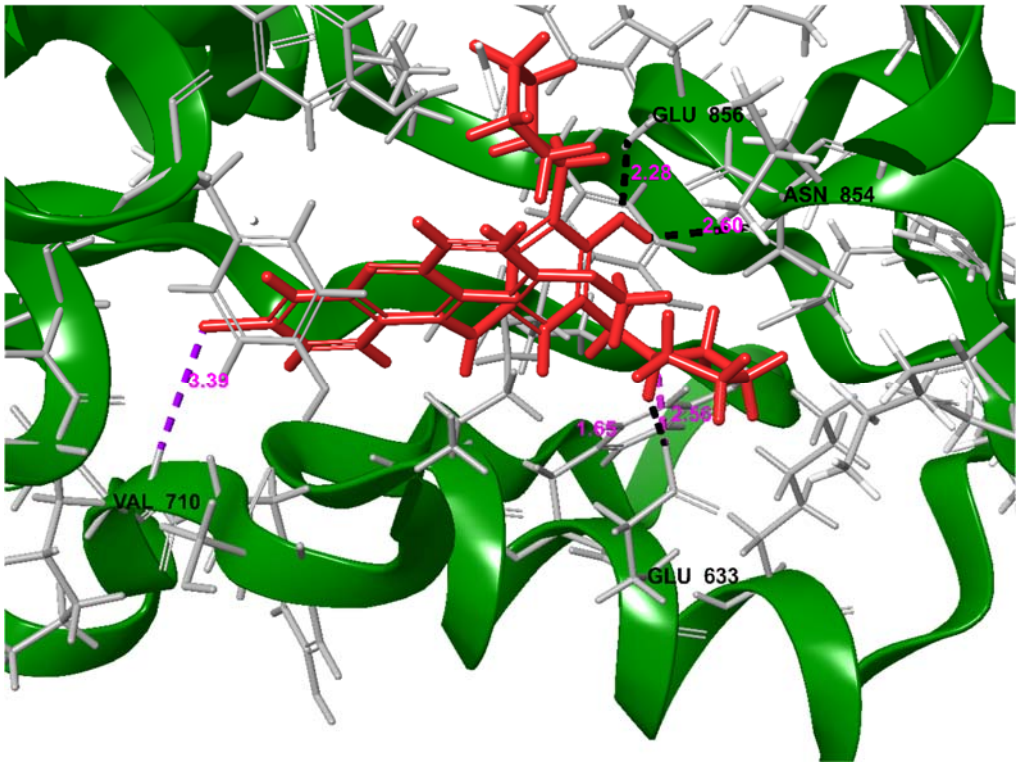

Figure SI.20: Binding pose and schematic representation of the interactions pyronaridine makes with surrounding residues of the DNA topoisomerase II enzyme

Abdissa, D., Geleta, G., Bacha, K., Abdissa, N., 2017. Phytochemical investigation of Aloe pulcherrima roots and evaluation for its antibacterial and antiplasmodial activities. PLOS ONE 12(3), e0173882.

Abegaz, B.M., Kebede, T., 1995. Geshoidin: A bitter principle of Rhamnus prinoides and other constituents of the leaves. Bulletin of the Chemical Society of Ethiopia 9(2).

Canche-Escamilla, G., Colli-Acevedo, P., Borges-Argaez, R., Quintana-Owen, P., May-Crespo, J.F., Cáceres-Farfan, M., Yam Puc, J.A., Sansores-Peraza, P., Vera-Ku, B.M., 2019. Extraction of phenolic components from an Aloe vera (Aloe barbadensis Miller) crop and their potential as antimicrobials and textile dyes. Sustainable Chemistry and Pharmacy 14, 100168.

Ngan, N.T.T., Quang, T.H., Kim, K.-W., Kim, H.J., Sohn, J.H., Kang, D.G., Lee, H.S., Kim, Y.-C., Oh, H., 2017. Anti-inflammatory effects of secondary metabolites isolated from the marine-derived fungal strain Penicillium sp. SF-5629. Archives of Pharmacal Research 40(3), 328-337.

Uzun, M., Guvenalp, Z., Kazaz, C., Demirezer, L.O., 2020. Matrix metalloproteinase inhibitor and sunscreen effective compounds from Rumex crispus L.: isolation, identification, bioactivity and molecular docking study. Phytochemical Analysis 31(6), 818-834.

Yagi, A., Makino, K., Nishioka, I., 1977. Studies on the Constituents of Aloe saponaria HAW. II. The Structures of Tetrahydroanthracene Derivatives, Aloesaponol III and -IV. CHEMICAL & PHARMACEUTICAL BULLETIN 25(7), 1764-1770.